

TOPOLOGY-AWARE GRAPH AUGMENTATION FOR PREDICTING CLINICAL TRAJECTORIES IN NEUROCOGNITIVE DISORDERS

Qianqian Wang¹, Wei Wang², Yuqi Fang¹, Hong-Jun Li², Andrea Bozoki³, Mingxia Liu^{1,*}

¹Department of Radiology and BRIC, University of North Carolina at Chapel Hill, NC 27599, USA

²Department of Radiology, Beijing Youan Hospital, Capital Medical University, Beijing, China

³Department of Neurology, University of North Carolina at Chapel Hill, NC 27599, USA

ABSTRACT

Brain networks/graphs derived from resting-state functional MRI (fMRI) help study underlying pathophysiology of neurocognitive disorders by measuring neuronal activities in the brain. Some studies utilize learning-based methods for brain network analysis, but typically suffer from low model generalizability caused by scarce labeled fMRI data. As a notable self-supervised strategy, graph contrastive learning helps leverage auxiliary unlabeled data. But existing methods generally arbitrarily perturb graph nodes/edges to generate augmented graphs, without considering essential topology information of brain networks. To this end, we propose a topology-aware graph augmentation (TGA) framework, comprising a *pretext model* to train a generalizable encoder on large-scale unlabeled fMRI cohorts and a *task-specific model* to perform downstream tasks on a small target dataset. In the pretext model, we design two novel topology-aware graph augmentation strategies: (1) *hub-preserving node dropping* that prioritizes preserving brain hub regions according to node importance, and (2) *weight-dependent edge removing* that focuses on keeping important functional connectivities based on edge weights. Experiments on 1,688 fMRI scans suggest that TGA outperforms several state-of-the-art methods.

Index Terms— Graph augmentation, Graph topology, Functional MRI

1. INTRODUCTION

Brain networks/graphs derived from resting-state functional MRI (fMRI) help objectively study underlying pathophysiology of neurocognitive disorders by measuring brain neuronal activities. Some fMRI-based studies utilize learning-based approaches for brain network analysis and imaging biomarker identification. But existing methods often suffer from poor model generalizability due to limited labeled data [1].

As a promising self-supervised learning strategy, graph contrastive learning provides an effective solution to pretrain a generalizable encoder on auxiliary data without requiring task-specific labels [2]. In general, it first performs graph data augmentation for each input graph to generate two views, and

then optimizes the agreement of graph representations from these two views to achieve self-supervised model training [3]. However, existing studies typically randomly perturb graph nodes or edges to generate augmented graphs for contrastive learning [4], ignoring the crucial topological information conveyed in functional brain networks.

To this end, we propose a topology-aware graph augmentation (TGA) framework for clinical trajectory prediction of HIV-associated neurocognitive disorders (HAND) with resting-state fMRI. As shown in Fig. 1, the TGA consists of a *pretext model* to train a generalizable graph convolutional network (GCN) encoder on large-scale unlabeled fMRI cohorts and a *task-specific model* to fine-tune the encoder for HIV-associated disorder identification and clinical score prediction on a target HAND dataset. We design two novel topology-aware graph augmentation strategies including (1) *hub-preserving node dropping* that prioritizes preserving brain hub regions according to node importance, and (2) *weight-dependent edge removing* that focuses on keeping important functional connectivities based on edge weights. Experiments on 1,688 fMRI scans validate the superiority of our TGA in classification and regression tasks. The TGA incorporates a learnable attention mask to automatically detect HIV-related brain regions and functional connectivities, providing potential imaging biomarkers for early intervention.

2. MATERIALS AND METHODOLOGY

2.1. Subjects and fMRI Preprocessing

Two publicly available cohorts (ABIDE [5] and MDD [6]) and a private HAND dataset with resting-state fMRI are used. From ABIDE and MDD, we select subjects whose time series length is at least 230, yielding 1,591 auxiliary fMRI scans for self-supervised model training. The HAND dataset is acquired from a local hospital, including 68 patients with HIV who exhibit asymptomatic neurocognitive impairment (ANI) and 69 age-matched healthy controls (HC). All fMRI scans are preprocessed using a standard pipeline [7].

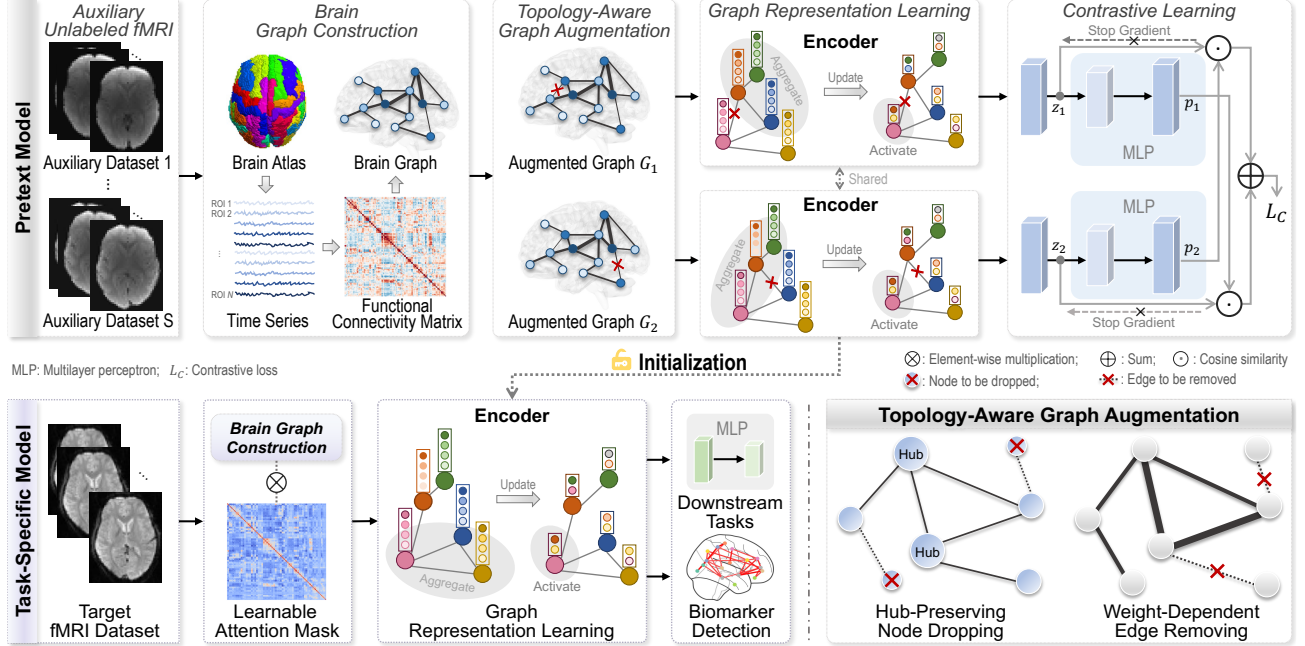


Fig. 1: Illustration of the proposed topology-aware graph augmentation (TGA) framework for functional MRI analysis.

2.2. Proposed Method

2.2.1. Pretext Model

Learning-based models generally suffer from poor generalization since labeled fMRI data is limited [1]. Inspired by [4], we design a *self-supervised pretext model* by leveraging large-scale unlabeled fMRI data to train a generalizable encoder that can well adapt to downstream tasks. As shown in the top panel of Fig. 1, with auxiliary unlabeled fMRI as input, the pretext model contains the following 4 components.

(1) Brain Graph Construction. A brain network derived from resting-state fMRI of a subject can be treated as a graph $G = \{V, E\}$, where $V = \{v_i\}_{i=1}^N$ is a set of ROIs/nodes, $E = \{e_{i,j}\}_{i,j=1}^N$ is a set of functional connectivities/edges, and N is the number of ROIs. We define the preprocessed fMRI time series as $S \in \mathbb{R}^{T \times N}$, where T is the length of time series. For each graph, we generate an adjacency matrix $A \in \mathbb{R}^{N \times N}$ by computing Pearson’s correlation (PC) between time series of paired ROIs. In this work, we denote node feature matrix as $X = A$, where the initial feature is connectivity strength between a node and all other nodes.

(2) Topology-Aware Graph Augmentation. To facilitate self-supervised training of the pretext model, we design two topology-aware graph augmentation methods that preserve graph topology information, driven by the prior that topological structure is crucial for analyzing functional pathology.

Hub-preserving Node Dropping (HND), which prioritizes preserving brain hub structure according to node importance. Here, we use degree centrality (DC) d_i to measure the importance of node v_i , and assign dropping probability to each node based on its DC. To prioritize preserving hub regions,

nodes with higher DC would have lower dropping probability. That is, the node dropping probability is inversely proportional to its centrality. The probability of a node v_i being dropped can be defined as $q_i = 1/d_i$. To obtain the probability distribution for HND, we perform probability normalization, represented as $p_i = q_i / \sum_{i=1}^N q_i$. Finally, we drop a certain proportion/ratio (*i.e.*, α) of nodes following this probability distribution to generate two augmented graphs G_i ($i = 1, 2$).

Weight-dependent Edge Removing (WER), which focuses on keeping important functional connectivities based on edge weights. Similar to HND, we define the probability for an edge $e_{i,j}$ being removed as $p_{i,j} = q_{i,j} / \sum_{i=1}^N \sum_{j=1}^N q_{i,j}$, where $q_{i,j} = 1/a_{i,j}$ and $a_{i,j}$ is the edge weight between node v_i and v_j . Here, we employ PC to describe functional connectivity strength (*i.e.*, edge weight). Likewise, we remove a certain proportion (*i.e.*, β) of edges to generate augmented graphs G_i ($i = 1, 2$) following this probability distribution for edge set. In this work, the node dropping ratio α and edge removing ratio β are empirically set as 10% and 50%, respectively.

(3) Graph Representation Learning. Considering the superiority of GCN in fMRI feature learning, the augmented graphs G_1 and G_2 are fed into two shared GCN encoders (two GCN layers with hidden dimension of 64 for each encoder) that can aggregate and update neighboring node features to generate new representations, described as:

$$Z = f(A, X) = \sigma(\hat{A}\sigma(\hat{A}XW^0)W^1), \quad (1)$$

where $\hat{A} = D^{-\frac{1}{2}}AD^{-\frac{1}{2}}$ is a normalized adjacency matrix, σ is *ReLU*, W^0 and W^1 are weight matrices, and D is a degree matrix. We then average over all rows of node feature matrix Z to generate a graph-level representation z_i ($i = 1, 2$).

Table 1: Results (%) of eight methods in the task of ANI vs. HC classification on the HAND dataset.

Method	AUC \uparrow	ACC \uparrow	SEN \uparrow	SPE \uparrow	BAC \uparrow
SVM	61.7(3.2)	57.3(2.7)	58.3(4.3)	57.2(2.9)	57.7(2.7)
XGBoost	56.7(3.6)	53.3(2.8)	51.7(3.6)	56.7(6.6)	54.2(2.8)
GCN	64.2(2.1)	59.6(2.3)	58.7(5.1)	61.7(4.9)	60.2(2.4)
GAT	65.7(3.9)	61.1(3.0)	62.5(5.8)	59.5(6.0)	61.0(0.1)
BrainNetCNN	65.4(1.6)	61.9(1.4)	61.7(3.7)	63.7(2.9)	62.7(1.1)
BrainGNN	63.0(3.2)	60.3(2.6)	56.3(6.0)	63.7(5.6)	60.0(1.8)
TGAN (Ours)	67.1(2.1)	60.5(3.8)	60.9(6.6)	60.9(6.4)	60.9(4.2)
TGAE (Ours)	69.9(3.5)	62.4(3.4)	60.2(5.7)	65.3(9.1)	62.8(3.2)

(4) Contrastive Learning. With z_1 and z_2 as input, we further apply multilayer perceptron (MLP) for feature abstraction, yielding two new representation vectors p_1 and p_2 . Following contrastive learning paradigms [2], our *pretext model* is updated by maximizing the similarity between two augmentation views from the same subject. Mathematically, the graph contrastive loss in our TGA can be formulated as:

$$\mathcal{L}_C = \Psi(\psi(z_1), p_2) + \Psi(\psi(z_2), p_1), \quad (2)$$

where Ψ is the negative cosine similarity. And ψ denotes the stop-gradient operation to ensure that the GCN encoder on G_1 receives no gradient from z_1 in the first term, but it receives gradients from p_1 in the second term (and vice versa for G_2), helping prevent model collapse [2].

2.2.2. Task-Specific Model

Our goal is to train a generalizable GCN encoder that can well adapt to the task-specific model. In the task-specific model, we first construct brain graphs based on target fMRI, and then feed these graphs into a GCN encoder for graph representation learning, followed by an MLP for prediction. Note that this encoder is initialized using parameters learned in the *pretext model*. In this work, we perform HIV-associated disorder classification and clinical score regression tasks, using cross-entropy loss and mean absolute error loss to fine-tune this task-specific model, respectively. To enhance interpretability of TGA, we incorporate a *learnable attention mask* M to automatically detect discriminative brain ROIs and functional connectivities. This is achieved by replacing the original \hat{A} in Eq. (1) with $\hat{A} \otimes M$, where \otimes is element-wise multiplication.

3. EXPERIMENTS

3.1. Experimental Setting

When using the proposed HND and WER strategies for graph augmentation, our methods are called **TAGN** and **TAGE**, respectively. In the experiments, we compare our methods with two traditional methods (*i.e.*, **SVM/SVR** and **XGBoost**) that use 464-dimensional node statistics as input, and four state-of-the-art (SOTA) deep learning methods (*i.e.*, **GCN** [8], **GAT** [9], **BrainNetCNN** [10], and **BrainGNN** [11]).

A 5-fold cross-validation strategy is used. In each fold, 80% of data is used for fine-tuning while 20% of data is used

Table 2: Regression results achieved by eight methods for predicting attention/working memory scores on HAND.

Method	MAE \downarrow	MSE \downarrow	PCC \uparrow
SVR	0.1767 \pm 0.0081	0.0485 \pm 0.0039	0.1091 \pm 0.0297
XGBoost	0.1511 \pm 0.0034	0.0381 \pm 0.0019	0.1340 \pm 0.0245
GCN	0.1577 \pm 0.0069	0.0421 \pm 0.0033	0.1502 \pm 0.0481
GAT	0.1556 \pm 0.0010	0.0410 \pm 0.0006	0.0920 \pm 0.0238
BrainNetCNN	0.1647 \pm 0.0091	0.0457 \pm 0.0050	0.1451 \pm 0.0298
BrainGNN	0.1610 \pm 0.0022	0.0418 \pm 0.0010	0.1413 \pm 0.0500
TGAN (Ours)	0.1477 \pm 0.0031	0.0373 \pm 0.0011	0.1819 \pm 0.0527
TGAE (Ours)	0.1464\pm0.0020	0.0363\pm0.0011	0.1952\pm0.0297

for validation. Five metrics are used for classification: area under ROC curve (AUC), accuracy (ACC), sensitivity (SEN), specificity (SPE), and balanced accuracy (BAC). Three metrics are used for regression: mean absolute error (MAE), mean squared error (MSE), and PC coefficient (PCC).

3.2. Result and Analysis

(1) Classification and Regression Results. We report the results achieved by eight methods in classification and regression tasks in Table 1 and Table 2, respectively. It can be observed from Table 1 that our methods generally show notable superiority over the traditional SVM and XGBoost methods in the classification task. The AUC of our TGAE is 13.2% higher than XGBoost in distinguishing ANI from HC. Compared with four SOTA methods (*e.g.*, BrainGNN), our methods yield better performance in most metrics. In addition, we can see from Table 2, our methods generally outperform six competing methods in cognitive score regression. These findings imply that our methods can learn discriminative graph representations in the two downstream tasks.

(2) Ablation Study. We compare TGAN and TGAE with 5 variants: **Naive** trained on the target cohort without the pretext model, **TGAN-F** and **TGAE-F** that directly apply the pretrained GCN encoder to the task-specific model without fine-tuning, **TGANw/tA** and **TGAEw/tA** without the learnable attention mask, with results reported in Fig. 2. From Fig. 2, TGAN and TGAE are superior to the Naive, validating the necessity of utilizing auxiliary fMRI for model pre-training when dealing with small-scale target data. Besides, our methods generally outperform frozen counterparts (*i.e.*, TGAN-F and TGAE-F), indicating that fine-tuning can enhance the adaptability of the pretrained encoder to target data. Additionally, our methods generally outperform TGANw/tA and TGAEw/tA in most cases, suggesting the effectiveness of the attention mask in learning discriminative graph features.

(3) Discriminative Functional Connectivity. In Fig. 3, we visualize the top 10 discriminative functional connectivities (FCs) identified by our method (with line width denoting attention weight) in ANI vs. HC classification. Figure 3 suggests that several ROIs are commonly detected in the identified FCs, including *orbital part of superior frontal gyrus*, *temporal pole of superior temporal gyrus*, and *superior tem-*

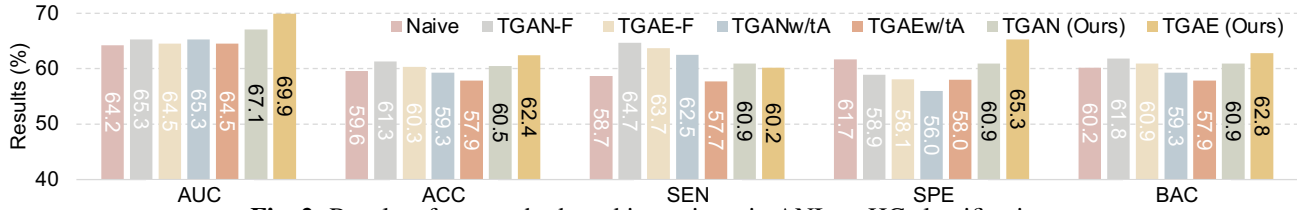


Fig. 2: Results of our methods and its variants in ANI vs. HC classification.

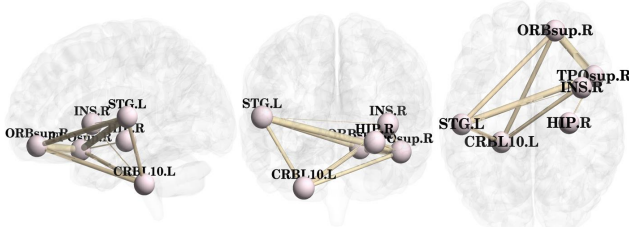


Fig. 3: Top 10 most discriminative functional connectivities in the ANI vs. HC classification task.

poral gyrus. This aligns with previous HIV-associated observations. These results demonstrate that the FCs and ROIs detected by our method have good interpretability, which can be used as potential imaging biomarkers for early identification of HIV-associated neurological changes.

4. CONCLUSION

This work presents a topology-aware graph augmentation (TGA) framework for fMRI analysis. The TGA comprises a pretext model trained on auxiliary unlabeled fMRI cohorts and a task-specific model fine-tuned on a target dataset. Two novel topology-aware graph augmentations are designed to facilitate self-supervised training. Experiments suggest the effectiveness of TGA in classification and regression tasks.

5. REFERENCES

[1] H. Cui, W. Dai, Y. Zhu, X. Li, L. He, and C. Yang, “Interpretable graph neural networks for connectome-based brain disorder analysis,” in *MICCAI*. Springer, 2022, pp. 375–385.

[2] X. Chen and K. He, “Exploring simple Siamese representation learning,” in *CVPR*, 2021, pp. 15750–15758.

[3] K. Hassani and A. Khasahmadi, “Contrastive multi-view representation learning on graphs,” in *ICML*. PMLR, 2020, pp. 4116–4126.

[4] Y. You, T. Chen, Y. Sui, T. Chen, Z. Wang, and Y. Shen, “Graph contrastive learning with augmentations,” *NeurIPS*, vol. 33, pp. 5812–5823, 2020.

[5] A. Di Martino, C. Yan, Q. Li, E. Denio, F. Castellanos, K. Alaerts, J. Anderson, M. Assaf, S. Bookheimer, M. Dapretto, et al., “The autism brain imaging data exchange: Towards a large-scale evaluation of the intrinsic brain architecture in autism,” *Molecular Psychiatry*, vol. 19, no. 6, pp. 659–667, 2014.

[6] C. Yan, X. Chen, L. Li, F. Castellanos, T. Bai, Q. Bo, J. Cao, G. Chen, N. Chen, W. Chen, et al., “Reduced default mode network functional connectivity in patients with recurrent major depressive disorder,” *PNAS*, vol. 116, no. 18, pp. 9078–9083, 2019.

[7] C. Yan and Y. Zang, “DPARSF: A MATLAB toolbox for “pipeline” data analysis of resting-state fMRI,” *Frontiers in Systems Neuroscience*, vol. 4, pp. 13, 2010.

[8] T. Kipf and M. Welling, “Semi-supervised classification with graph convolutional networks,” *arXiv preprint arXiv:1609.02907*, 2016.

[9] P. Velivković, G. Cucurull, A. Casanova, A. Romero, P. Lio, and Y. Bengio, “Graph Attention Networks,” *arXiv preprint arXiv:1710.10903*, 2017.

[10] J. Kawahara, C. Brown, S. Miller, B. Booth, V. Chau, R. Grunau, J. Zwicker, and G. Hamarneh, “Brain-NetCNN: Convolutional neural networks for brain networks; towards predicting neurodevelopment,” *NeuroImage*, vol. 146, pp. 1038–1049, 2017.

[11] Xiaoxiao Li, Yuan Zhou, Nicha Dvornek, Muhan Zhang, Siyuan Gao, Juntang Zhuang, Dustin Scheinost, Lawrence H Staib, Pamela Ventola, and James S Duncan, “BrainGNN: Interpretable brain graph neural network for fMRI analysis,” *Medical Image Analysis*, vol. 74, pp. 102233, 2021.